



Cite this: DOI: 10.1039/d0em00244e

## Complexation by cysteine and iron mineral adsorption limit cadmium mobility during metabolic activity of *Geobacter sulfurreducens*†

E. J. Tomaszewski,<sup>ID</sup>\*<sup>ab</sup> L. Olson,<sup>a</sup> M. Obst,<sup>ID</sup><sup>c</sup> J. M. Byrne,<sup>ID</sup><sup>ad</sup> A. Kappler,<sup>ID</sup><sup>a</sup> and E. M. Muehe,<sup>ID</sup><sup>ae</sup>

Cadmium (Cd) adversely affects human health by entering the food chain *via* anthropogenic activity. In order to mitigate risk, a better understanding of the biogeochemical mechanisms limiting Cd mobility in the environment is needed. While Cd is not redox-active, Cd speciation varies (*i.e.*, aqueous, complexed, adsorbed), and influences mobility. Here, the cycling of Cd in relation to initial speciation during the growth of *Geobacter sulfurreducens* was studied. Either fumarate or ferrihydrite (Fh) was provided as an electron acceptor and Cd was present as: (1) an aqueous cation, (2) an aqueous complex with cysteine, which is often present in metal stressed soil environments, or (3) adsorbed to Fh. During microbial Fe(III) reduction, the removal of Cd was substantial (~80% removal), despite extensive Fe(II) production (ratio Fe(II)<sub>total</sub> : Fe<sub>total</sub> = 0.8). When fumarate was the electron acceptor, there was higher removal from solution when Cd was complexed with cysteine (97–100% removal) compared to aqueous Cd (34–50%) removal. Confocal laser scanning microscopy (CLSM) demonstrated the formation of exopolymeric substances (EPS) in all conditions and that Cd was correlated with EPS in the absence of Fe minerals ( $r = 0.51$ – $0.56$ ). Most notable is that aqueous Cd was more strongly correlated with *Geobacter* cells ( $r = 0.72$ ) compared to Cd–cysteine complexes ( $r = 0.51$ ). This work demonstrates that Cd interactions with cell surfaces and EPS, and Cd solubility during metabolic activity are dependent upon initial speciation. These processes may be especially important in soil environments where sulfur is limited and Fe and organic carbon are abundant.

Received 1st June 2020  
Accepted 9th August 2020

DOI: 10.1039/d0em00244e

rsc.li/espi

### Environmental significance

Cadmium (Cd) in phosphorus-based fertilizers is mobile in soils and can bioaccumulate in crops. Long-term consumption of contaminated food causes several health problems. Therefore, it is imperative that factors controlling the mobility and biogeochemical cycling of Cd in soils are understood. Here, we demonstrate that initial speciation (aqueous, complexed or adsorbed) directly impacts the fate of Cd during microbial metabolism, influencing the extent of Cd removal from solution, and the association of Cd with biomass, as shown using confocal laser scanning microscopy. This work highlights the importance of metal speciation in relation to microbial metabolism and trace metal fate, even in cases of non-redox active metals.

### Introduction

Cadmium (Cd) is a toxic, non-redox-active metal that can enter soils through the use of low-quality phosphate fertilizers,<sup>1–3</sup> and/or anthropogenic waste, such as mining and smelting

waste.<sup>4,5</sup> Due to its relatively stable electronic configuration as Cd<sup>2+</sup> ([Kr] 4s<sup>2</sup> 3d<sup>10</sup>), Cd does not readily oscillate between oxidation states in the environment. Once in soils, Cd can bioaccumulate in plants, including foodstuffs such as rice and wheat.<sup>6,7</sup> The consumption of Cd leads to a wide variety of health problems, the most infamous of which is itai-itai disease, which emerged in Japan in the 1940's and 50's. This disease induces extreme spinal deformation and pain, caused by the substitution of calcium by Cd into human bone.<sup>8,9</sup> Today, Cd contamination is once again a human health issue, especially in China where Cd soil concentrations range from 0.003 to 9.57 mg kg<sup>−1</sup>.<sup>4</sup>

There are many constituents of soil matrices with which Cd can interact, such as carbonate minerals, sulfide minerals and iron (Fe) (oxyhydr)oxide minerals.<sup>7,10–13</sup> Recently, the solubility

<sup>a</sup>Geomicrobiology Group, Center for Applied Geoscience (ZAG), University of Tübingen, Schnarrenbergstrasse 94-96, Tübingen, D-72076, Germany. E-mail: ejtomas@udel.edu

<sup>b</sup>University of Delaware, 221 Academy St, Newark, DE 19716, USA

<sup>c</sup>Experimental Biogeochemistry, BayCEER, University Bayreuth, Dr.-Hans-Frisch-Str. 1-3, Bayreuth, 95448, Germany

<sup>d</sup>School of Earth Sciences, University of Bristol, Queens Road, Bristol, BS8 1QU, UK

<sup>e</sup>Plant Biogeochemistry Group, Department Environmental Microbiology, Helmholtz-Centre for Environmental Research, Leipzig, Germany

† Electronic supplementary information (ESI) available. See DOI: 10.1039/d0em00244e

of Cd has been closely linked to the transformation of transition metal (oxyhydr)oxides, highlighting the importance of these phases for Cd biogeochemical cycling in soils.<sup>12</sup> In addition to limiting solubility, the adsorption of Cd onto phases such as ferrihydrite (Fh) ( $\text{Fe}_{10}\text{O}_{14}(\text{OH})_2$ ) can also limit the bioavailability of Cd to certain plant species.<sup>14</sup> Fe(III)-reducing bacteria, such as *Geobacter sulfurreducens*, play an important role not only in the biogeochemical cycling of Fe and carbon in soil environments, but also of trace metals and metalloids, such as chromium (Cr) and arsenic (As), that may be adsorbed to high surface area, reactive Fe minerals. There have been many studies which examine microbial Fe metabolism in relation to Cr and As,<sup>15–18</sup> but relatively few examining the fate of Cd during microbial Fe metabolism.<sup>13,19</sup>

In addition to adsorption processes with Fe(III) (oxyhydr)oxides and other mineral phases, Cd can also form aqueous phase complexes with organic matter (OM)<sup>3</sup> and smaller organic carbon molecules such as cysteine.<sup>20</sup> Cysteine is a small amino acid that is often associated with metallothionein proteins that are active *in vivo* in removing heavy metals *via* the thiol moiety.<sup>20</sup> Cadmium can form complexes with cysteine *via* this moiety and the presence of cysteine can mitigate Cd toxicity for microbial species such as *Escherichia coli* and tobacco plant species.<sup>21,22</sup> This thiol moiety is also capable of binding other chalcophilic metals such as mercury (Hg) and the complexation of Hg with cysteine has been linked to higher rates of cellular uptake and methylation in *G. sulfurreducens* and other species.<sup>23,24</sup> The fate of Cd when complexed with cysteine during the metabolic processes of *G. sulfurreducens* remains poorly understood.

Understanding the fate of Cd during microbial metabolic processes is important because the interaction of this heavy metal with biomass can have profound effects on its solubility and mobility. Although some heavy metals can be used as a terminal electron acceptor<sup>25,26</sup> and metal-responsive genes are present in *G. sulfurreducens*,<sup>27</sup> this microbial species can still be subject to heavy metal stress and toxicity. Microorganisms exhibit several types of stress response pathways toward heavy metals, such as exportation out of cells or intra/extracellular complexation. Heavy metals may inhibit the metabolic activity of soil microbes, which can alter the extent of carbon cycling and lead to the accumulation of OM at the surface soils.<sup>28</sup> This change in carbon cycling could directly impact the fate of Cd by leading to increased Cd-OM complexation and/or formation of mineral surface ternary Cd-OM complexes.<sup>3,29</sup> Other possible stress responses of microbial species to heavy metals include the formation of poorly soluble metal complexes, the binding of metals to cells walls or proteins and the production of exopolymeric substances (EPS) as sorbents to lower the dissolved concentration of the toxic metal.<sup>28</sup>

The goal of this work was to examine how the initial speciation of Cd can influence the mobility of this metal during metabolic activity. The initial Cd species studied included: (1) aqueous Cd, (2) Cd complexed with cysteine and (3) Cd adsorbed to ferrihydrite. Cysteine was used as a small organic molecule for Cd complexation due to the fact that it is often produced by plants<sup>30,31</sup> and/or present on important metal detoxification metallothionein proteins.<sup>32,33</sup> *G. sulfurreducens*

was exposed to these different Cd species while growing on either acetate and fumarate or acetate and the Fe(III) mineral ferrihydrite.

## Methods

### Microbial cultivation

*Geobacter sulfurreducens* strain PCA was grown in a 22 mM  $\text{HCO}_3^-$  pH 7.0 buffered growth medium, containing  $\text{NH}_4\text{Cl}$  (5.5 mM),  $\text{MgSO}_4 \cdot 7\text{H}_2\text{O}$  (2 mM),  $\text{KH}_2\text{PO}_4$  (3.5 mM),  $\text{CaCl}_2 \cdot 2\text{H}_2\text{O}$  (0.68 mM) and NaCl (3.45 mM). Supplements added for growth include a selenium tungstate solution (SeW),<sup>34</sup> a trace element solution,<sup>35</sup> and a 7-vitamin solution.<sup>36</sup> Growth medium was prepared anoxically and under sterile conditions according to Widdel *et al.*<sup>34</sup> During pre-culture growth, acetate (25 mM) was supplied as an electron donor and fumarate (40 mM) as an electron acceptor. Cultures were grown for 5 days until the late log phase, in the dark at 30 °C prior to inoculation for microcosm experiments. Separate stock cultures were used for Fe and fumarate microcosms, containing  $2.7 \times 10^8$  cells per mL for Fe microcosm experiments and  $1.2 \times 10^8$  cells per mL for fumarate microcosm experiments, as determined by flow cytometry.

### Microcosm experiments

For Fe microcosm experiments, ferrihydrite was synthesized by rapidly titrating 0.5 M ferric chloride ( $\text{FeCl}_3$ ) with 1 M KOH to a final pH of 7, while not exceeding pH 7.5. The resulting slurry was centrifuged and resuspended four times with deionized water. After the last centrifugation step, ferrihydrite was resuspended in ultrapure water ( $18.2 \text{ M}\Omega \text{ cm}^{-1}$ ) in a 100 mL glass serum vial. The vial was sealed with a butyl stopper the headspace was exchanged with  $\text{N}_2$ . The stock concentration of the ferrihydrite was verified *via* dissolution in 6 M HCl and analysis using the ferrozine method.<sup>37</sup>

Microcosm experiments were growth experiments, where changes in either gene copy numbers or cell numbers were measured. Fe microcosm experiments were prepared in triplicate in 50 mL glass serum bottles, which were sterilized *via* acid washing (1 M HCl) and baking (4 h, 180 °C) prior to use. The medium used was a 10 mM PIPES (1,4 piperazinediethanesulfonic acid) buffered growth medium (pH 6.8), containing the same ions, trace metals and nutrients as the pre-culture growth medium with the exception of  $\text{KH}_2\text{PO}_4$  which was reduced from 3.5 mM to 0.05 mM, to limit precipitation of Cd with  $\text{PO}_4$ , a change which also influences the precipitation of Fe(II) phases. Acetate (10 mM), ferrihydrite (10 mM) and Cd as  $\text{CdCl}_2$  (100  $\mu\text{M}$  or 11  $\text{mg L}^{-1}$ ) were added to serum vials 24 hours prior to inoculation with cells. This concentration of Cd was chosen for Fe microcosms because it has been previously demonstrated *Geobacter sulfurreducens* tolerates this concentration of Cd without the expense of diminishing Fe(III) reduction.<sup>13</sup> Furthermore, 100  $\mu\text{M}$  Cd gives rise to an aqueous/bioavailable amount of Cd often found in the environment.<sup>19</sup> After 24 hours,  $82 \pm 1.2\%$  of the added Cd was adsorbed to the Fe solid. *Geobacter sulfurreducens* cells ( $2.7 \times 10^7$  cells per mL) were then added to microcosms for a total of 40 mL and

incubated in the dark at 30 °C for 14 days. Microcosm reactors were sampled in an anoxic chamber (MBraun; 100% N<sub>2</sub>) to preserve Fe(II) during sampling.

For microcosm experiments where fumarate was used as the electron acceptor (*i.e.*, no Fe present), the same growth medium as described for Fe microcosms was employed and reactors were also prepared in 50 mL sterile glass serum vials, in triplicate. Acetate (25 mM) was used as the electron donor and fumarate (40 mM) was used as the electron acceptor. Cadmium was added to microcosms 24 hours prior to inoculation with cells, either in the presence or absence of 2 mM cysteine, ensuring all reactants were in serum vials before cell addition. Cysteine was in excess compared with Cd (20 times more cysteine) to ensure complete complexation of Cd would occur and no other possible ligands were present prior to inoculation with cells. Two different Cd concentrations were tested in fumarate microcosm experiments, 5.6 mg L<sup>-1</sup> (50 μM) or 11 mg L<sup>-1</sup> (100 μM) in order to account for the likely intolerance of *Geobacter sulfurreducens* to Cd in the absence of Fe. After 24 hours, *Geobacter sulfurreducens* cells (1.2 × 10<sup>7</sup> cells per mL) were added to microcosms for a total of 40 mL and incubated in the dark at 30 °C for 14 days. Microcosms were sampled in a sterile and anoxic manner on the bench top.

### Analytical methods

For Fe microcosm experiments, samples for aqueous Fe(II) analysis were centrifuged for 10 minutes at 14 000 rpm in the anoxic chamber and the supernatant was then diluted in 1 M HCl. The remaining supernatant was discarded and the solid pellet was dissolved in 6 M HCl in order to determine total Fe and solid Fe(II). Prior to bringing the samples outside of the anoxic chamber, samples were diluted in 1 M HCl to avoid Fe(II) oxidation by O<sub>2</sub>.<sup>38</sup> The concentration of Fe in all of the aforementioned samples was measured using the ferrozine method.<sup>37</sup> 16S rRNA gene copy quantities were determined by extracting DNA from samples stored at -20 °C using the DNeasy Power Soil kit (QIAGEN) according to the manufacturers protocol and quantitative polymerase chain reaction (q-PCR) and analysis with SsoAdvanced Universal SYBR Green Supermix (Bio-Rad-Laboratories, Hercules, CA, USA) using a q-PCR cyclor (Bio-Rad, Hercules, CA, USA). This method was chosen due to the limited interference with Fe minerals during analysis. The supernatant from centrifuged samples was used for aqueous Cd quantification. Aqueous Cd was determined using microwave plasma atomic emission spectroscopy (MP-AES) (Agilent 4200). For fumarate microcosm experiments, cell numbers were determined using flow cytometry. Briefly, samples (3 μL) were prepared under sterile conditions in sterilized Eppendorf tubes with 10 mM PIPES buffer (194 μL) and BactLight green dye (2 μL) (Thermo Fischer). Samples (65 μL) were then pipetted into a 96-well plate and analyzed in technical, as well as biological triplicates, along with positive (cells from stock cultures) and negative controls (PIPES buffer only). For aqueous Cd, samples were centrifuged (14 000 rpm, 10 minutes) and Cd concentration was determined from the supernatant using MP-AES.

### Confocal laser scanning microscopy and data analysis

For confocal laser scanning microscopy (CLSM) experiments, separate duplicate microcosm reactors were prepared. All pre-culture growth conditions and experimental conditions were as similar as possible to previous microcosm experiments. Aqueous Cd geochemistry results from microcosm experiments for CLSM experiments are shown in Fig. S1.† Only one concentration of Cd (11 mg L<sup>-1</sup>) was used in the fumarate cultures for these experiments, to ensure Cd detection would not be an issue and to have similar concentration between fumarate and Fe cultures for this analysis.

Samples (100 μL) were taken from the aqueous phase of cultures and stained with 1 μL of two 1 mg mL<sup>-1</sup> Lectin-Alexa Fluor conjugate solutions, ConA-Alexa 633 (excitation 635 nm, detection 645–700 nm) and WGA-Alexa 555 (excitation 561 nm, detection 566–620 nm), as well as 1 μL of Syto 40 (excitation 405 nm, detection 420–480 nm). The ConA-Alexa 633 is expected to stain alpha-mannopyranosyl and alpha-glucopyranosyl compounds, and WGA-Alexa 55 is expected to stain *N*-acetylglucosamine and *N*-acetylneuraminic acid residues. The Syto 40 stain reacts with DNA and is used to visualize cells. Samples were not taken from any biofilms on the bottom of vials. After a 20 minute incubation period, 1 μL of the 1 mg mL<sup>-1</sup> Cd-sensitive fluorescence dye (Heliosense, HS010-002-1, excitation 488 nm, emission 500–550 nm) was added and samples were incubated for an additional two minutes. For control samples with no Cd, a dilution of 1 : 10 was used for the Cd heliosense dye to sample in order to minimize fluorescence interference from the background. Samples from Fe cultures were stained in an anoxic chamber with a N<sub>2</sub> atmosphere. Image stacks (44 × 44 μm with 1024 × 1024 pixels) were obtained in sequential mode using an upright Leica TCS SPE system equipped with four solid state lasers (405, 488, 456, 635 nm) with an ACS APO 63× water immersion CS objective (Leica Microsystems, Wetzlar, Germany). The reflection signal was measured using the 488 nm laser. The pinhole was set to 0.5 Airy units to optimize lateral and axial resolution at the cost of fluorescence intensity. The pixel size of 42.7 × 42.7 nm<sup>2</sup> ensures Nyquist sampling at the optical resolution limit of the system and allows for high quality correlation analysis. Five to six image stacks were acquired for each sample condition. Blind deconvolution was applied to all 3D image stacks using the Auto-Quant™ deconvolution algorithm without background subtraction and rescaling. Fiji, an open source image analysis software (<https://fiji.sc/>), was used for data handling, visualization and statistical analysis.<sup>39,40</sup> Scatterplots for correlation analysis were made using the ScatterJ plugin.<sup>41</sup>

## Results and discussion

### Cd geochemistry during microbial Fe(III) reduction

The percentages of Cd removed from solution in all setups is relative to the initial total Cd measured (Fig. S2.†). In Fe microcosm experiments, after the first day of incubation with cells, 97 ± 0% of the total Cd was removed from solution (Fig. 1); however, in the abiotic control (*i.e.*, no cells), only 79 ± 3% of the total Cd

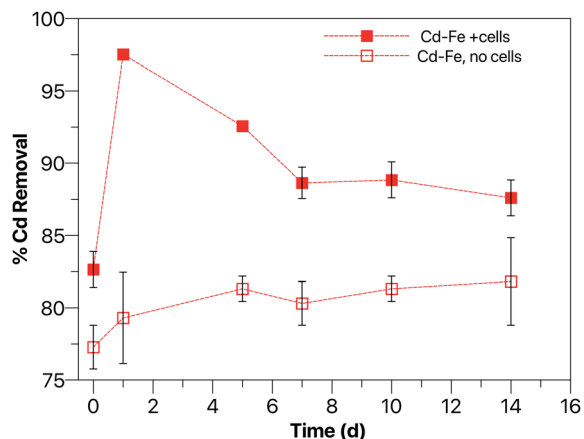


**Fig. 1** Removal of Cd (%) from solution in Fe microcosm experiments. Cd–Fh + cells (closed red squares) represents microcosms where 11 mg L<sup>-1</sup> Cd was initially primarily adsorbed to Fh and *Geobacter sulfurreducens* cells were added. Day 0 was taken before the addition of cells. Cd–Fh, no cells (open red squares) represents microcosms where no cells were added to reactors containing Cd adsorbed to Fh. Error bars represent standard deviation of triplicate reactors.

was removed after the first 24 hours. As a result of microbial Fe(III) reduction, an increase of Fe(II)<sub>total</sub> : Fe<sub>total</sub> (from 0 to 0.05 ± 0.003) was observed, which could have led to a Fe(II) catalyzed transformation of ferrihydrite to initially more crystalline phases, such as goethite (α-FeOOH) or magnetite (Fe<sub>3</sub>O<sub>4</sub>) (Fig. 2). Mineral transformation would likely decrease the surface area as well as the adsorption capacity of the mineral phase,<sup>42,43</sup> such that an increase in aqueous Cd is expected, and thus, a lower % removal of Cd from solution. However, the opposite trend in Cd behavior was observed, with an initial increase in the % removal of Cd in the first 24 hours of incubation (Fig. 1). Therefore, this increase in

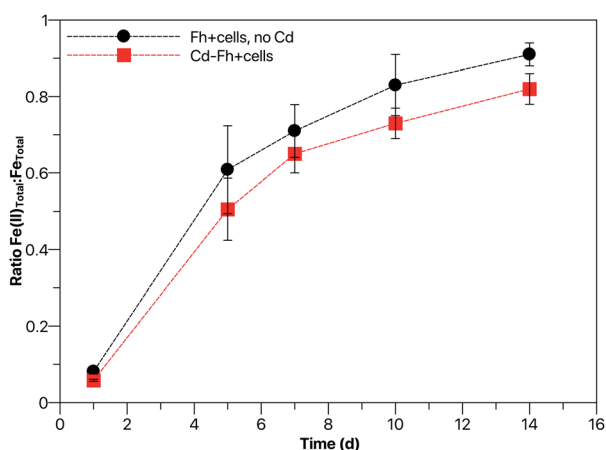


**Fig. 2** Ratio of total Fe(II) : total Fe during microbial Fe(III) reduction by *Geobacter sulfurreducens*. Fh + cells, no Cd (black circles) represents microcosms with *Geobacter sulfurreducens* cells and Fh but no Cd. Cd–Fh + cells (red squares) represents microcosms where 11 mg L<sup>-1</sup> Cd was initially primarily adsorbed to Fh and *Geobacter sulfurreducens* cells were added. Fe(II) and Fe total were quantified via the ferrozine method. Error bars represent the standard deviation of triplicate reactors.

% removal of Cd is more likely due to an interaction with biomass, rather than the mineral phase, as discussed later.

Throughout the experiment, the extent of Cd removal decreased from 97 ± 0% at day 1 to 87 ± 1.2% at day 14 (Fig. 1). During this Cd release, the ratio of Fe(II)<sub>total</sub> : Fe<sub>total</sub> steadily increased, reaching 0.82 ± 0.04 in the presence of Cd by day 14 (Fig. 2). This considerable microbial Fe(III) reduction lead to mineral transformation (based on color change observations, Fig. S3†) and a small release of Cd into solution. Following extensive microbial Fe(III) reduction, less than 15% (12.4% ± 1.2) of Cd was detected in solution after 14 days (Fig. 1). Further examination of the aqueous Cd species measured (*i.e.*, determining aqueous Cd–organic carbon phases, Cd–PO<sub>4</sub><sup>3-</sup> or Cd–CO<sub>3</sub><sup>2-</sup> complexes) was not performed. Calculations using Visual MINTEQ demonstrated the majority (*ca.* 80%) of Cd would be present as Cd<sup>2+</sup> or CdCl<sup>+</sup> at equilibrium in the absence of cysteine. Only 12% of Cd would be present as an aqueous CdHPO<sub>4</sub><sup>-</sup> complex and the remaining Cd species would be less than 5% each. The precipitation of CdCO<sub>3</sub> is expected to be minimal at equilibrium. While speciation is certainly important, here we focused on understanding how initial speciation ultimately influences solubility and interactions with biomass. This limited concentration of aqueous Cd is similar to what has been observed in microbial Fe(III) reduction experiments with other *Geobacter* species, *Geobacter metallireducens* GS-15 and *Geobacter* sp. Cd1, a Cd resistant strain.<sup>13</sup> In comparison to these two strains, more microbial Fe(III) reduction occurred when *Geobacter sulfurreducens* was used in this study, with 82 ± 4% observed here compared to ~20–70% previously.<sup>13</sup> It must be noted that higher initial cell numbers (2.7 × 10<sup>7</sup> cells per mL) were used in this growth study compared to the previous study (5 × 10<sup>5</sup>–10<sup>6</sup> cells per mL), which could be one reason why a higher extent of microbial Fe(III) reduction occurred here. Nevertheless, it is interesting that a similar trend in aqueous Cd behavior was observed for both *Geobacter* sp. Cd1 and *Geobacter sulfurreducens* during microbial Fe(III) reduction in this study, despite the differences in initial cell numbers and differences in the extent of microbial Fe(III) reduction.<sup>13</sup> These findings here highlight that Fe minerals are a strong sink for Cd, even under highly reduced conditions, despite the fact that incorporation of Cd into the lattice structure of Fe(III) (oxyhydr)oxides is in theory limited due to the relatively large hydrated ionic radius of Cd(II) (95 pm), compared to that of Fe(II) (78 pm) and Fe(III) (65 pm).<sup>44</sup>

### The mobility of Cd in the presence and absence of cysteine

In addition to Cd adsorbed to ferrihydrite, two other initial Cd species, at two different Cd concentrations (5.6 and 11 mg L<sup>-1</sup>), were examined during the growth of *Geobacter sulfurreducens* using fumarate as an electron acceptor: aqueous Cd and Cd complexed with cysteine. As stated, two different concentrations of Cd were used in fumarate microcosms because the Cd tolerance was expected to be lower in the absence of Fe.

In microcosms containing initially aqueous Cd without cysteine, there was a steady removal of Cd from solution from day 1 to 5 when the total Cd concentration was 11 mg L<sup>-1</sup>

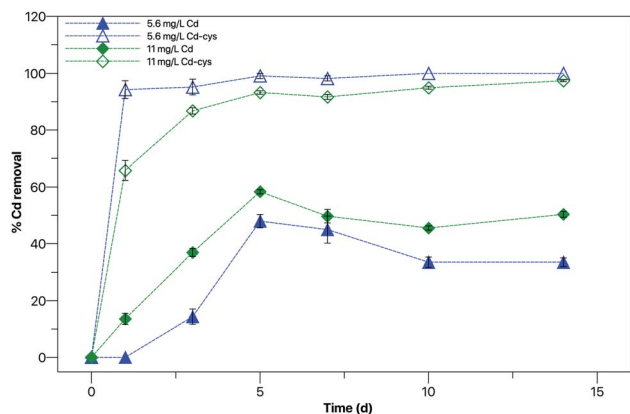


Fig. 3 Removal of Cd from solution during the growth of *Geobacter sulfurreducens* when Cd was initially an aqueous cation (blue triangles, green diamonds) and complexed with cysteine (open blue triangles, open green diamonds). All data shown is from reactors with cells. Abiotic controls (no cells) are shown in ESI (Fig. S4†). Samples for day 0 were taken before the addition of cells. Cd concentrations were quantified with MP-AES. Error bars represent standard deviation of triplicate reactors.

(Fig. 3). However, after day 5 only an average of  $48 \pm 2.6\%$  of the total Cd was removed from solution. In microcosms containing  $5.6 \text{ mg L}^{-1}$  Cd, Cd removal from solution did not begin until day 3, reached  $48 \pm 2.3\%$  by day 5 but stabilized at  $33 \pm 1.5\%$  by day 10 (Fig. 3). At both concentrations of aqueous Cd, after day 5 when the amount of Cd removed from solution began to decrease, cell numbers also began to decrease (Fig. 4). One theory behind this correlation is that potentially cells lysed due to toxicity effects, which liberated 8–14% Cd ( $\leq 1.12 \text{ mg L}^{-1}$ ) into solution (Fig. 3). This process would mean aqueous Cd was highly available to biomass during the first five days of growth. Therefore, Cd was in proximity of cell surfaces, allowing for adsorption to cell walls or potentially cellular uptake, both of which will be discussed further later. The release of Cd after initial removal was not observed in microcosms with Cd–cysteine complexes, and therefore it seems when Cd is initially present as an aqueous cation it is more mobile during microbial

metabolism compared to when it is initially present as an aqueous cysteine-complex.

Conversely, when Cd was initially complexed with cysteine, regardless of the initial concentration, extensive and rapid removal of Cd from solution was observed during incubation with cells, with  $94 \pm 3.1\%$  Cd removal in microcosms with  $5.6 \text{ mg L}^{-1}$  Cd and  $65 \pm 3.4\%$  of Cd removal in microcosms with  $11 \text{ mg L}^{-1}$  Cd after 1 day (Fig. 3). By the end of the 14 day incubation, 97–100% Cd removal was measured in all microcosms containing Cd–cysteine complexes, regardless of concentration. Microcosm reactors were well mixed prior to sampling, and abiotic controls did not show the same near complete removal of Cd from solution in the presence of cysteine, occurring by day 3 (Fig. S4†). Therefore, there is a clear combined effect of Cd complexation with cysteine and subsequent interaction with biomass on the removal of Cd from solution. One possibility for the extensive removal of Cd in this system is the formation of CdS nanoparticles. Studies have shown microbial species such as *Escherichia coli* can enzymatically degrade cysteine to produce dissolved sulfide, which in turn forms nanoparticles with chalcophilic metals such as Hg.<sup>45–47</sup> Specifically, the production of 13–20  $\mu\text{M}$  sulfide by *G. sulfurreducens* in the presence of 100–1000  $\mu\text{M}$  cysteine led to the precipitation of HgS nanoparticulate phases.<sup>46</sup> Here, we used a much higher concentration of cysteine (2 mM), which has been shown to limit HgS precipitation at 50 nM Hg concentrations.<sup>45</sup> While our concentrations of cysteine and Cd were higher than these studies, we cannot rule out the possibility that CdS nanoparticles formed and became associated with biomass (*i.e.*, cells and/or EPS), contributing to the extensive removal of Cd from solution. Other potential removal mechanisms are discussed further below.

#### Potential cellular adsorption and uptake of Cd

There are several potential mechanisms which may be responsible for the removal of Cd from solution in all three experimental setups investigated here. First, the adsorption of Cd to cell walls can occur through carboxyl, phosphoryl, sulfhydryl or hydroxyl functional groups present on cell surfaces.<sup>48–51</sup> At

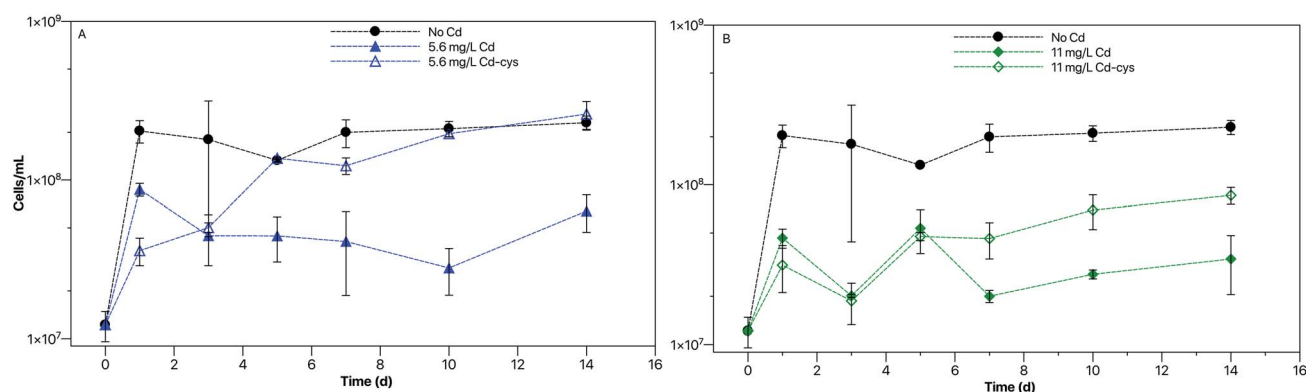


Fig. 4 Cellular growth as demonstrated by *Geobacter sulfurreducens* cell numbers. Panels (A) and (B) represents data from reactors with  $5.6 \text{ mg L}^{-1}$  and  $11 \text{ mg L}^{-1}$  Cd, respectively. Cell numbers were determined using flow cytometry and results shown are from triplicate reactors. Error bars represent standard deviations.

pH 6.8, it is expected that carboxyl ( $pK_a \cong 4.6$ ) and phosphoryl ( $pK_a \cong 6.6$ ) groups are to some extent deprotonated and are therefore the major functional groups able to bind Cd.<sup>49,52</sup> At low metal loadings (*i.e.*, 25  $\mu\text{mol Cd/g}$  bacteria), sulfhydryl groups have been shown to be responsible for nearly all of Cd binding to cells, even though these sites only comprise 5% of total available sites.<sup>53–55</sup> However, in the systems discussed here, the metal loading is beyond the range where sulfhydryl groups have been shown to dominate Cd adsorption processes to cells and are therefore not considered in these present calculations. The equilibrium constants for the binding of Cd by carboxyl and phosphoryl functional groups has already been established using potentiometric techniques, and the total site concentrations are calculated based on the cell numbers (1 cell =  $10^{-12}$  g) and carboxyl and phosphoryl site densities.<sup>49,56</sup> These site densities for cell walls are not specific to *G. sulfurreducens* but to Gram-negative bacteria, that in theory should have similar cell surface structures. In order to calculate the concentration of Cd adsorbed to cells, we used the equilibrium expression shown in eqn (1) and assumed literature site density values.

$$K_{\text{ads}} = \frac{[\text{R} - \text{S}_i - \text{M}^+]}{\alpha_{\text{M}^{2+}} [\text{R} - \text{S}_i^-]} \quad (1)$$

Here,  $K_{\text{ads}}$  is the equilibrium constant for Cd binding with carboxyl or phosphoryl functional groups,  $[\text{R} - \text{S}_i - \text{M}^+]$  is the concentration of Cd bound,  $\alpha_{\text{M}^{2+}}$  is the activity of Cd and  $[\text{R} - \text{S}_i^-]$  is the concentration of binding sites. Gene copy numbers from the Fe microcosm experiments (Fig. S5†) were used to estimate cell numbers during growth. When the amount of Cd adsorption to cell surfaces was calculated for Fe microcosm experiments,  $<1 \mu\text{M}$  Cd likely was bound the cell surface. Therefore, although Cd adsorption to cell surfaces was possible, these calculations suggest it was not the dominant mechanism driving Cd cycling during microbial Fe(III) reduction at this concentration investigated. However, correlation analysis from CLSM results demonstrates there exists a slight correlation between Cd and the cells, visualized by the Syto-40 stain ( $r = 0.43 \pm 0.06$ ) (Fig. 5). From these experiments, however, we cannot conclude whether the functional groups binding Cd are associated with the outer membrane, lipopolysaccharides or a closely bound glycocalyx around the cell. To better understand Cd-cell associations, an additional CLSM experiment was performed using a lipid membrane specific dye (FM-4-64,  $1 \text{ mg L}^{-1}$ ; Thermo Fisher Scientific) and is discussed further below.

Another mechanism by which Cd could be removed from solution is *via* cellular uptake. Cell growth relative to cultures without Cd suggests that cellular uptake of Cd was either limited in Fe microcosm experiments or that the concentration taken up was not extremely toxic (Fig. 2 and S5†). When comparing 16S rRNA gene copy numbers of *Geobacter sulfurreducens* during microbial Fe(III) reduction in the presence of  $11 \text{ mg L}^{-1}$  Cd and in the absence of Cd, there was a minimal difference (Fig. S5†). There was clear growth in both sets of cultures after 24 hours of incubation, increasing from  $2.7 \times 10^7$  to  $1.2 \times 10^8$  gene copies per mL in the absence of Cd and to  $2.3 \times 10^8$  gene copies per mL in the presence of Cd (Fig. S5†).

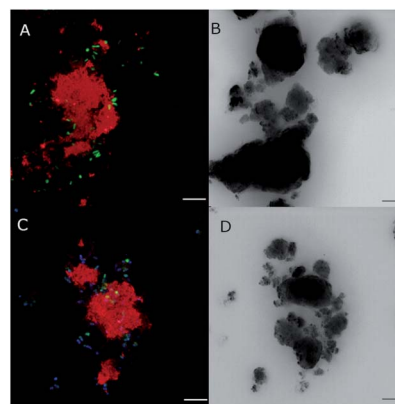


Fig. 5 Confocal laser scanning microscopy images of samples taken from Fe microcosms without Cd (A and B) and with Cd (C and D). Colored images represent fluorescence channels, with the sum of ConA and WGA lectins in red, the Syto 40 stain in green and the Cd heliosense stain in blue. Black and white images are transmission data of the same area wherein the contrast is dominated by the absorbance of the Fe-minerals. Scale bars are 5  $\mu\text{m}$ .

Furthermore, the ratio of  $\text{Fe(II)}_{\text{total}} : \text{Fe}_{\text{total}}$  in microcosms with and without Cd was similar throughout the 14 day experiment (Fig. 2), indicating the presence of Cd did not greatly affect the rate or extent of microbial Fe(III) reduction. Whether or not cellular uptake of  $1.7 \text{ mg L}^{-1}$  or 10% of total Cd occurred after 24 hours of inoculation is unclear, but the trends in metabolic activity suggest that the toxic effects of Cd were minimal with respect to growth during microbial Fe(III) reduction of ferrihydrite.

In microcosms where Cd was initially present as either an aqueous cation or complexed with cysteine, the concentration of Cd adsorbed to cell walls was calculated to be  $<2 \mu\text{M}$  throughout the 14 day experiment. Therefore, at the concentrations of Cd investigated, adsorption to cell walls was not expected to be the primary mechanism of Cd removal from solution. However, the correlation between Cd and cells was stronger compared to Fe cultures and the extent of this correlation depends on the initial speciation of Cd. For example, in the aqueous Cd cultures, Cd positively correlated with cells ( $r = 0.72 \pm 0.02$ ) and micrographs illustrated a diffusion of Cd throughout the image (Fig. 6). Individual cells were less noticeable than in the Cd-cysteine system, as was the Syto 40 stain (shown in green) in general. The Syto 40 stain is active with both DNA and RNA; thus, the depleted green color in these images could elude to decreased microbial activity. This decrease in microbial activity and DNA aligns with lower cell numbers in aqueous Cd cultures and further illustrates the toxic effect of aqueous Cd. Conversely, Cd correlated with cells in Cd-cysteine cultures ( $r = 0.51 \pm 0.05$ ), and these cultures demonstrated higher cell numbers compared to aqueous Cd counterparts. CLSM analysis, in conjunction with flow cytometry data, shows that the complexation of Cd with cysteine leads to better growth of *G. sulfurreducens* compared to the system with initially aqueous Cd, as well as a lower association of Cd with microbial cells.

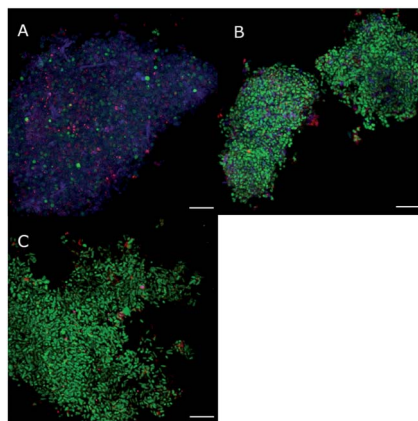


Fig. 6 Confocal scanning laser microscopy images from fumarate cultures with difference initial Cd species, aqueous Cd (A), Cd complexed with cysteine (B) and no Cd (C). The sum of ConA and WGA lectin stains are shown in red, the Syto 40 stain is shown in green and the Cd Heliosense stain is shown in blue. Scale bars are 5  $\mu\text{m}$ .

Similar to the Fe cultures, the association of Cd with cells could also be a result of the cellular uptake of Cd when fumarate is the electron acceptor. For example, the complexation of cysteine with metals such as mercury (Hg) and Cd can increase cellular uptake of metals into microbial and phytoplankton cells.<sup>23,57</sup> Specifically, when Hg was bound to cysteine, the extent of Hg uptake and rate of methylation were both significantly higher for *G. sulfurreducens* compared to when Hg was bound to other thiols.<sup>23</sup> Thus, because Hg and Cd are in the same group in the periodic table it is possible that these metals have similar chemical behavior and potentially similar mechanisms of cellular uptake strategies by *G. sulfurreducens*. If this mechanism of Cd removal was occurring, it would mean that the toxic effects of Cd were somehow neutralized when complexed with cysteine and taken up by cells because cell growth continued throughout the 14 day experiment (Fig. 4). In fact, microcosms containing Cd–cysteine complexes had a longer lag phase at both 5.6 and 11  $\text{mg L}^{-1}$  but clear growth trends were observed, with cell numbers reaching  $2.6 \times 10^8$  cells per mL and  $8.6 \times 10^7$  cells per mL respectively (Fig. 4). Cellular concentrations of Cd were not measured, but by estimating the density of cells (*ca.*  $0.25 \mu\text{m}^3$  per cell), the theoretical concentration of Cd in a cell was calculated to be  $840\,000 \text{ mg L}^{-1}$  (750 mM) if all of the Cd was taken up in the 5.6  $\text{mg L}^{-1}$  Cd reactors, for example, illustrating that complete uptake was impossible.

Although complete cellular uptake of Cd was impossible, an additional CLSM experiment demonstrated a clear association of Cd with cellular lipid membranes (Fig. S12 and S13<sup>†</sup>). The FM-4-64 stain, specific to lipid membranes, was used in conjunction with the Cd Heliosense dye. In Fig. S12,<sup>†</sup> clear rings of Cd around cell walls are visible and there is a distinct correlation between Cd and the lipid membranes. Pearson's correlation analysis demonstrated a strong correlation between Cd and FM-4-64 ( $r = 0.87$ ), as well as Cd and cells ( $r = 0.66$ ) (Fig. S13<sup>†</sup>). Conversely, the correlation between FM-4-64 and the Syto 40 stain was not as strong as the other two at an  $r$  value of 0.35. These correlation analyses illustrate that, although the

concentration of Cd bound to cell wall functional groups was not calculated to be high, some Cd was clearly bound to cell walls or to the closely bound glycocalyx. Furthermore, the CLSM data confirms that there was likely little Cd within the cells, but rather Cd surrounding cell structures.

### The production and adsorption capacity of EPS

The final potential mechanism of Cd removal from solution discussed here is the adsorption of Cd to EPS, which is likely an important mechanism in all systems studied. EPS have a three-dimensional, gel-like and highly hydrated structure which can be comprised of polysaccharides, proteins, nucleic acids and phospholipids.<sup>58,59</sup> In the environment biofilms and flocs are formed primarily of EPS and even in laboratory conditions EPS production has been measured. Thus, EPS production seems to be an important feature of survival, as many bacteria occur as flocs and in biofilms<sup>58–60</sup> and may be particularly important in the presence of toxic metals. EPS have similar carboxyl, phosphoryl and sulfhydryl binding sites for Cd as cell surfaces and binding site concentrations have been reported in some cases to be 20–30 higher on EPS compared to cell surfaces.<sup>53,61</sup> In addition to these binding sites, protein and polysaccharide content have also been shown to be important factors in the removal of Cd from solution.<sup>52</sup> When *G. sulfurreducens* was previously grown on fumarate, the production of EPS was quantified during both the exponential and stationary phase and was determined to be made up primarily of proteins and carbohydrates.<sup>62</sup>

Fluor Alexa stains ConA and WGA were used to stain glycoconjugates and the sum of these fluorescence channels (*via* Fiji) was used to represent a major fraction of EPS produced by these cells. It must be noted that these lectin stains likely do not stain all EPS but it is a good approximation.<sup>63</sup> From CLSM analysis, it is clear EPS is produced by *G. sulfurreducens* across all three starting Cd conditions, as well as in Cd-free controls (Fig. 5 and 6). In the Fe cultures, there was not a strong correlation between EPS and Cd ( $r = 0.31 \pm 0.08$ ) and it is clear from visual inspection of CLSM images that the majority of the Cd was associated with the Fe minerals and not directly with either cells nor necessarily EPS (Fig. 5). EPS was clearly observed associated with the Fe minerals (Fig. 5), as expected.<sup>63</sup> Nevertheless, the additional removal of Cd in Fe cultures compared to the abiotic control can still be attributed to association with biomass, even though the adsorption of Cd onto cell walls was calculated to be minimal and there was not a strong correlation between Cd and EPS. For example, in the Fe system, a  $15 \pm 1.2\%$  increase in Cd removal from solution was observed after the first 24 hours of inoculation with cells, compared to only a  $2 \pm 1.6\%$  increase in abiotic controls. Additional adsorption sites provided by EPS for Cd could have contributed to the removal of Cd from solution, even though there is not a strong correlation between Cd and EPS in Fe cultures.

In the fumarate cultures, EPS was clearly present (Fig. 6) but qualitatively more was observed in the Fe cultures. Thus, the production of EPS by *G. sulfurreducens* is not necessarily in direct response to the presence of Cd; however, the chemical

structure of the EPS produced may be different in the presence of Cd and this merits further investigation. For example, in cultures with Cd–cysteine complexes, a strong biofilm formed on the bottom of the serum vials after 1 day of growth and this was not broken up during sampling. This biofilm that formed Cd–cysteine reactors was in addition to the dense suspension of biomass, from which CLSM samples were taken. It is important to note that cysteine was in excess in relation to Cd in order to ensure complete complexation of Cd. It was suggested that Cd can form bidentate complexes with cysteine at circumneutral pH;<sup>20</sup> thus 1.8–1.9 mM cysteine is still available to be used by microbes for other purposes, such as biomass production and detoxification. Cysteine in particular is an important residue on proteins responsible for heavy metal detoxification in both plants and microbial species.<sup>21,64</sup> Therefore, in the environment, it is possible that excess cysteine may be produced by plant species and a microbial community, not only limiting the mobility of Cd but also providing excess cysteine to species such as *G. sulfurreducens*. The excess cysteine in this system could have been used in the formation of a robust biofilm and/or EPS with sulfhydryl groups, which could have contributed to the extensive removal (97–100%) of Cd in this system (Fig. 3). There exists a slight correlation between Cd and EPS in these cultures ( $r = 0.56 \pm 0.05$ ), as well as in aqueous Cd cultures ( $r = 0.51 \pm 0.04$ ), suggesting that EPS was adsorbing some Cd. When a correlation analysis was done for individual lectin stains vs. Cd, there was more of difference between the aqueous Cd and Cd–cysteine systems, specifically with respect to the WGA stain. The WGA stain specifically targets *N*-acetylglucosamine and *N*-acetylneuraminic acid residues.<sup>63</sup> In the Cd–cysteine system, WGA vs. Cd correlation analysis produced an  $r$  value of  $0.43 \pm 0.04$ ; however, in the aqueous Cd system,  $r = 0.19 \pm 0.02$ . It is clear that Cd–cysteine complexes are interacting differently with lectins, which could be influencing overall toxicity and mobility.

## Conclusions

While Cd is not a redox-active metal, this work illustrates that different geochemical species of Cd can have different fates during microbial metabolism. When initially adsorbed to a poorly crystalline Fe(III) (oxyhydr)oxide such as ferrihydrite, >85% of the total Cd in the system remained associated with the solid phase, even when ~80% of the Fe(III) underwent microbial Fe(III) reduction. The extent of this reduction may differ in the environment, where different microbial species are present and individual strain cell numbers differ; however, this work demonstrates how strong the interaction between Cd and Fe minerals can be, even during extensive ( $82 \pm 3\%$ ) Fe(III) reduction. Furthermore, this Cd–Fe mineral interaction appears to ameliorate some of the toxic effects of Cd toward *Geobacter sulfurreducens*, given that 16S rRNA gene copy numbers do not change dramatically during growth in the presence of adsorbed Cd.

In addition to the fate of Cd with Fe minerals during microbial Fe(III) reduction, the fate of Cd complexed with cysteine and aqueous Cd during the reduction of fumarate was

also examined. From this work, it is clear that cysteine increased the rate and extent of Cd removal from solution, with 97–100% removal regardless of the initial starting concentration. Although an increased lag phase was observed, microbial growth prevailed in the Cd–cysteine system, especially compared to the aqueous Cd system. Finally, CLSM data demonstrated different degrees of correlation of Cd with cells and EPS depending on the initial Cd speciation. Aqueous Cd was more highly correlated with microbial cells and in the presence of cysteine, the correlation of Cd with *N*-acetylglucosamines was stronger. Overall, it is clear that cysteine and Fe(III) minerals can limit Cd mobility during microbial metabolism, though the specific molecular biological mechanistic details of these phenomena remain unclear.

## Conflicts of interest

There are no conflicts to declare.

## Acknowledgements

This work was funded by the DFG, via proposal KA 1736/55-1. We would like to thank several people for their assistance and contributions to this manuscript. Ellen Röhm for analyzing MP-AES samples, as well as general laboratory assistance, Julian Sorwat for MP-AES analysis, Lars Grimm for assistance with microbial culturing and flow cytometry, Franziska Schädler for assistance with DNA extraction and q-PCR and Antonia Freiburger for her assistance with CLSM sample preparation and data collection. The CLSM experiments were supported by the DFG grant OB362/4-1; Martin Obst was supported by the DFG grant OB362/3-1.

## References

- 1 E. Smolders and J. Mertens, Cadmium, in *Heavy Metals in Soils*, B. J. Alloway, Springer Netherlands, 2013, vol. 22, pp. 283–311, DOI: 10.1007/978-94-007-4470-7.
- 2 M. A. Khan, S. Khan, A. Khan and M. Alam, Soil Contamination with Cadmium, Consequences and Remediation Using Organic Amendments, *Sci. Total Environ.*, 2017, **601–602**, 1591–1605, DOI: 10.1016/j.scitotenv.2017.06.030.
- 3 I. D. Santos, S. L. Rodrigues, J. O. Siqueira, M. B. M. Monte and A. J. B. Dutra, Effect of Partial Oxidation of Organic Matter on Cadmium Leaching from Phosphate, *Miner. Eng.*, 2016, **99**, 67–75, DOI: 10.1016/j.mineng.2016.09.021.
- 4 L. Wang, X. Cui, H. Cheng, F. Chen, J. Wang, X. Zhao, C. Lin and X. Pu, A Review of Soil Cadmium Contamination in China Including a Health Risk Assessment, *Environ. Sci. Pollut. Res.*, 2015, **22**(21), 16441–16452, DOI: 10.1007/s11356-015-5273-1.
- 5 W.-J. Yang, K.-B. Ding, P. Zhang, H. Qiu, C. Cloquet, H.-J. Wen, J.-L. Morel, R.-L. Qiu and Y.-T. Tang, Cadmium Stable Isotope Variation in a Mountain Area Impacted by Acid Mine Drainage, *Sci. Total Environ.*, 2019, **646**, 696–703, DOI: 10.1016/j.scitotenv.2018.07.210.



- 6 M. Imseng, M. Wiggnerhauser, A. Keller, M. Müller, M. Rehkämper, K. Murphy, K. Kreissig, E. Frossard, W. Wilcke and M. Bigalke, Fate of Cd in Agricultural Soils: A Stable Isotope Approach to Anthropogenic Impact, Soil Formation, and Soil-Plant Cycling, *Environ. Sci. Technol.*, 2018, **52**(4), 1919–1928, DOI: 10.1021/acs.est.7b05439.
- 7 M. Furuya, Y. Hashimoto and N. Yamaguchi, Time-Course Changes in Speciation and Solubility of Cadmium in Reduced and Oxidized Paddy Soils, *Soil Sci. Soc. Am. J.*, 2016, **80**(4), 870, DOI: 10.2136/sssaj2016.03.0062.
- 8 M. Fleischer, A. F. Sarofim, D. W. Fassett, P. Hammond, H. T. Shacklette, I. C. Nisbet and S. Epstein, Environmental Impact of Cadmium: A Review by the Panel on Hazardous Trace Substances, *Environ. Health Perspect.*, 1974, **7**, 253–323.
- 9 K. Nogawa, E. Kobayashi, Y. Okubo and Y. Suwazono, Environmental Cadmium Exposure, Adverse Effects and Preventive Measures in Japan, *BioMetals*, 2004, **17**(5), 581–587, DOI: 10.1023/B:BIOM.0000045742.81440.9c.
- 10 S. Khaokaew, R. L. Chaney, G. Landrot, M. Ginder-Vogel and D. L. Sparks, Speciation and Release Kinetics of Cadmium in an Alkaline Paddy Soil under Various Flooding Periods and Draining Conditions, *Environ. Sci. Technol.*, 2011, **45**(10), 4249–4255, DOI: 10.1021/es103971y.
- 11 B. Fulda, A. Voegelin and R. Kretzschmar, Redox-Controlled Changes in Cadmium Solubility and Solid-Phase Speciation in a Paddy Soil As Affected by Reducible Sulfate and Copper, *Environ. Sci. Technol.*, 2013, **47**(22), 12775–12783, DOI: 10.1021/es401997d.
- 12 J. Wang, P.-M. Wang, Y. Gu, P. M. Kopittke, F.-J. Zhao and P. Wang, Iron–Manganese (Oxyhydro)Oxides, Rather than Oxidation of Sulfides, Determine Mobilization of Cd during Soil Drainage in Paddy Soil Systems, *Environ. Sci. Technol.*, 2019, **53**(5), 2500–2508, DOI: 10.1021/acs.est.8b06863.
- 13 E. M. Muehe, M. Obst, A. Hitchcock, T. Tyliczszak, S. Behrens, C. Schröder, J. M. Byrne, F. M. Michel, U. Krämer and A. Kappler, Fate of Cd during Microbial Fe(III) Mineral Reduction by a Novel and Cd-Tolerant Geobacter Species, *Environ. Sci. Technol.*, 2013, **47**(24), 14099–14109, DOI: 10.1021/es403365w.
- 14 C. E. Rosenfeld, R. L. Chaney and C. E. Martínez, Soil Geochemical Factors Regulate Cd Accumulation by Metal Hyperaccumulating *Noccaea Caerulescens* (J. Presl & C. Presl) F.K. Mey in Field-Contaminated Soils, *Sci. Total Environ.*, 2018, **616–617**(Supp. C), 279–287, DOI: 10.1016/j.scitotenv.2017.11.016.
- 15 C. Hohmann, E. Winkler, G. Morin and A. Kappler, Anaerobic Fe(II)-Oxidizing Bacteria Show As Resistance and Immobilize As during Fe(III) Mineral Precipitation, *Environ. Sci. Technol.*, 2010, **44**(1), 94–101, DOI: 10.1021/es900708s.
- 16 M. Herbel and S. Fendorf, Biogeochemical Processes Controlling the Speciation and Transport of Arsenic within Iron Coated Sands, *Chem. Geol.*, 2006, **228**(1–3), 16–32, DOI: 10.1016/j.chemgeo.2005.11.016.
- 17 B. D. Kocar, M. J. Herbel, K. J. Tufano and S. Fendorf, Contrasting Effects of Dissimilatory Iron(III) and Arsenic(V) Reduction on Arsenic Retention and Transport, *Environ. Sci. Technol.*, 2006, **40**(21), 6715–6721, DOI: 10.1021/es061540k.
- 18 C. M. Hansel, B. W. Wielinga and S. Fendorf, Structural and Compositional Evolution of Cr/Fe Solids after Indirect Chromate Reduction by Dissimilatory Iron-Reducing Bacteria, *Geochim. Cosmochim. Acta*, 2003, **67**(3), 401–412.
- 19 E. M. Muehe, I. J. Adaktylou, M. Obst, F. Zeitvogel, S. Behrens, B. Planer-Friedrich, U. Kraemer and A. Kappler, Organic Carbon and Reducing Conditions Lead to Cadmium Immobilization by Secondary Fe Mineral Formation in a PH-Neutral Soil, *Environ. Sci. Technol.*, 2013, **47**(23), 13430–13439, DOI: 10.1021/es403438n.
- 20 F. Jalilehvand, B. O. Leung and V. Mah, Cadmium(II) Complex Formation with Cysteine and Penicillamine, *Inorg. Chem.*, 2009, **48**(13), 5758–5771, DOI: 10.1021/ic802278r.
- 21 C. G. Kawashima, M. Noji, M. Nakamura, Y. Ogra, K. T. Suzuki and K. Saito, Heavy Metal Tolerance of Transgenic Tobacco Plants Over-Expressing Cysteine Synthase, *Biotechnol. Lett.*, 2004, **26**(2), 153–157, DOI: 10.1023/B:BILE.0000012895.60773.ff.
- 22 M. Wang, S. Duan, Z. Zhou and S. Chen, Alleviation of Cadmium Toxicity to Tobacco (*Nicotiana Tabacum*) by Biofertilizers Involves the Changes of Soil Aggregates and Bacterial Communities, *Ecotoxicol. Environ. Saf.*, 2019, **169**, 240–247, DOI: 10.1016/j.ecoenv.2018.10.112.
- 23 J. K. Schaefer and F. M. M. Morel, High Methylation Rates of Mercury Bound to Cysteine by *Geobacter Sulfurreducens*, *Nat. Geosci.*, 2009, **2**(2), 123–126, DOI: 10.1038/ngeo412.
- 24 J. An, L. Zhang, X. Lu, D. A. Pelletier, E. M. Pierce, A. Johs, J. M. Parks and B. Gu, Mercury Uptake by *Desulfovibrio Desulfuricans* ND132: Passive or Active?, *Environ. Sci. Technol.*, 2019, **53**(11), 6264–6272, DOI: 10.1021/acs.est.9b00047.
- 25 D. R. Lovley, S. J. Giovannoni, D. C. White, J. E. Champine, E. J. P. Phillips, Y. A. Gorby and S. Goodwin, *Geobacter Metallireducens* Gen. Nov. Sp. Nov., a Microorganism Capable of Coupling the Complete Oxidation of Organic Compounds to the Reduction of Iron and Other Metals, *Arch. Microbiol.*, 1993, **159**, 336–344.
- 26 D. R. Lovley, E. J. P. Phillips, Y. A. Gorby and E. R. Landa, Microbial Reduction of Uranium, *Nature*, 1991, **350**(6317), 413–416, DOI: 10.1038/350413a0.
- 27 B. A. Methé, K. E. Nelson, J. A. Eisen, I. T. Paulsen, W. Nelson, J. F. Heidelberg, D. Wu, M. Wu, N. Ward, M. J. Beanan, R. J. Dodson, R. Madupu, L. M. Brinkac, S. C. Daugherty, R. T. DeBoy, A. S. Durkin, M. Gwinn, J. F. Kolonay, S. A. Sullivan, D. H. Haft, J. Selengut, T. M. Davidsen, N. Zafar, O. White, B. Tran, C. Romero, H. A. Forberger, J. Weidman, H. Khouri, T. V. Feldblyum, T. R. Utterback, S. E. V. Aken, D. R. Lovley and C. M. Fraser, Genome of *Geobacter Sulfurreducens*: Metal Reduction in Subsurface Environments, *Science*, 2003, **302**(5652), 1967–1969, DOI: 10.1126/science.1088727.

- 28 N. Abdu, A. A. Abdullahi and A. Abdulkadir, Heavy Metals and Soil Microbes, *Environ. Chem. Lett.*, 2017, **15**(1), 65–84, DOI: 10.1007/s10311-016-0587-x.
- 29 M. B. Kirkham, Cadmium in Plants on Polluted Soils: Effects of Soil Factors, Hyperaccumulation, and Amendments, *Geoderma*, 2006, **137**(1), 19–32, DOI: 10.1016/j.geoderma.2006.08.024.
- 30 J. R. Domínguez-Solis, M. C. López-Martín, F. J. Ager, M. D. Ynsa, L. C. Romero and C. Gotor, Increased Cysteine Availability Is Essential for Cadmium Tolerance and Accumulation in *Arabidopsis thaliana*, *Plant Biotechnol. J.*, 2004, **2**(6), 469–476, DOI: 10.1111/j.1467-7652.2004.00092.x.
- 31 E. Harada and Y.-E. Choi, Investigation of Metal Exudates from Tobacco Glandular Trichomes under Heavy Metal Stresses Using a Variable Pressure Scanning Electron Microscopy System, *Plant Biotechnol.*, 2008, **25**(4), 407–411, DOI: 10.5511/plantbiotechnology.25.407.
- 32 G. Henkel and B. Krebs, Metallothioneins: Zinc, Cadmium, Mercury, and Copper Thiols and Selenols Mimicking Protein Active Site Features – Structural Aspects and Biological Implications, *Chem. Rev.*, 2004, **104**(2), 801–824, DOI: 10.1021/cr020620d.
- 33 Y. Boulanger, C. M. Goodman, C. P. Forte, S. W. Fesik and I. M. Armitage, Model for Mammalian Metallothionein Structure, *Proc. Natl. Acad. Sci. U. S. A.*, 1983, **80**(6), 1501–1505, DOI: 10.1073/pnas.80.6.1501.
- 34 F. Widdel and F. Bak, Gram-Negative Mesophilic Sulfate-Reducing Bacteria, in *The Prokaryotes: A Handbook on the Biology of Bacteria: Ecophysiology, Isolation, Identification, Applications*, ed. A. Balows, H. G. Trüper, M. Dworkin, W. Harder and K.-H. Schleifer, Springer New York, New York, NY, 1992, pp. 3352–3378, DOI: 10.1007/978-1-4757-2191-1\_21.
- 35 F. Widdel, G.-W. Kohring and F. Mayer, Studies on Dissimilatory Sulfate-Reducing Bacteria That Decompose Fatty Acids, *Arch. Microbiol.*, 1983, **134**(4), 286–294, DOI: 10.1007/BF00407804.
- 36 F. Widdel and N. Pfennig, Studies on Dissimilatory Sulfate-Reducing Bacteria That Decompose Fatty Acids, *Arch. Microbiol.*, 1981, **129**(5), 395–400, DOI: 10.1007/BF00406470.
- 37 L. L. Stookey, Ferrozine—a New Spectrophotometric Reagent for Iron, *Anal. Chem.*, 1970, **42**(7), 779–781.
- 38 K. Porsch and A. Kappler, FeII Oxidation by Molecular O<sub>2</sub> during HCl Extraction, *Environ. Chem.*, 2011, **8**(2), 190, DOI: 10.1071/EN10125.
- 39 J. Schindelin, I. Arganda-Carreras, E. Frise, V. Kaynig, M. Longair, T. Pietzsch, S. Preibisch, C. Rueden, S. Saalfeld, B. Schmid, J.-Y. Tinevez, D. J. White, V. Hartenstein, K. Eliceiri, P. Tomancak and A. Cardona, Fiji: An Open-Source Platform for Biological-Image Analysis, *Nat. Methods*, 2012, **9**(7), 676–682, DOI: 10.1038/nmeth.2019.
- 40 C. A. Schneider, W. S. Rasband and K. W. Eliceiri, NIH Image to ImageJ: 25 Years of Image Analysis, *Nat. Methods*, 2012, **9**(7), 671–675.
- 41 F. Zeitvogel, G. Schmid, L. Hao, P. Ingino and M. Obst, ScatterJ: An ImageJ plugin for the evaluation of analytical microscopy datasets, *Journal of Microscopy*, 2016, **261**(2), 148–156, DOI: 10.1111/jmi.12187.
- 42 H. D. Pedersen, D. Postma, R. Jakobsen and O. Larsen, Fast Transformation of Iron Oxyhydroxides by the Catalytic Action of Aqueous Fe(II), *Geochim. Cosmochim. Acta*, 2005, **69**(16), 3967–3977, DOI: 10.1016/j.gca.2005.03.016.
- 43 C. M. Hansel, S. G. Benner and S. Fendorf, Competing Fe(II)-Induced Mineralization Pathways of Ferrihydrite, *Environ. Sci. Technol.*, 2005, **39**(18), 7147–7153, DOI: 10.1021/es050666z.
- 44 Y. Marcus, Thermodynamics of Solvation of Ions, *J. Chem. Soc., Faraday Trans.*, 1991, **87**, 5.
- 45 S. A. Thomas, P. Catty, J.-L. Hazemann, I. Michaud-Soret and J.-F. Gaillard, The Role of Cysteine and Sulfide in the Interplay between Microbial Hg(II) Uptake and Sulfur Metabolism, *Metallomics*, 2019, **11**(7), 1219–1229, DOI: 10.1039/C9MT00077A.
- 46 S. A. Thomas, K. E. Rodby, E. W. Roth, J. Wu and J.-F. Gaillard, Spectroscopic and Microscopic Evidence of Biomediated HgS Species Formation from Hg(II)–Cysteine Complexes: Implications for Hg(II) Bioavailability, *Environ. Sci. Technol.*, 2018, **52**(17), 10030–10039, DOI: 10.1021/acs.est.8b01305.
- 47 S. A. Thomas and J.-F. Gaillard, Cysteine Addition Promotes Sulfide Production and 4-Fold Hg(II)–S Coordination in Actively Metabolizing *Escherichia Coli*, *Environ. Sci. Technol.*, 2017, **51**(8), 4642–4651, DOI: 10.1021/acs.est.6b06400.
- 48 N. Yee and J. Fein, Cd Adsorption onto Bacterial Surfaces: A Universal Adsorption Edge?, *Geochim. Cosmochim. Acta*, 2001, **65**(13), 2037–2042, DOI: 10.1016/S0016-7037(01)00587-7.
- 49 B. R. Ginn and J. B. Fein, The Effect of Species Diversity on Metal Adsorption onto Bacteria, *Geochim. Cosmochim. Acta*, 2008, **72**(16), 3939–3948, DOI: 10.1016/j.gca.2008.05.063.
- 50 J. B. Fein, C. J. Daughney, N. Yee and T. A. Davis, A Chemical Equilibrium Model for Metal Adsorption onto Bacterial Surfaces, *Geochim. Cosmochim. Acta*, 1997, **61**(16), 3319–3328, DOI: 10.1016/S0016-7037(97)00166-X.
- 51 M. I. Boyanov, S. D. Kelly, K. M. Kemner, B. A. Bunker, J. B. Fein and D. A. Fowle, Adsorption of Cadmium to *Bacillus Subtilis* Bacterial Cell Walls: A PH-Dependent X-Ray Absorption Fine Structure Spectroscopy Study, *Geochim. Cosmochim. Acta*, 2003, **67**(18), 3299–3311, DOI: 10.1016/S0016-7037(02)01343-1.
- 52 X. Wei, L. Fang, P. Cai, Q. Huang, H. Chen, W. Liang and X. Rong, Influence of Extracellular Polymeric Substances (EPS) on Cd Adsorption by Bacteria, *Environmental Pollution*, 2011, **159**(5), 1369–1374, DOI: 10.1016/j.envpol.2011.01.006.
- 53 J. B. Fein, Q. Yu, J. Nam and N. Yee, Bacterial Cell Envelope and Extracellular Sulfhydryl Binding Sites: Their Roles in Metal Binding and Bioavailability, *Chemical Geology*, 2019, **521**, 28–38, DOI: 10.1016/j.chemgeo.2019.04.026.
- 54 B. Mishra, M. I. Boyanov, B. A. Bunker, S. D. Kelly, K. M. Kemner, R. Nerenberg, B. L. Read-Daily and J. B. Fein, An X-Ray Absorption Spectroscopy Study of Cd

- Binding onto Bacterial Consortia, *Geochim. Cosmochim. Acta*, 2009, **73**(15), 4311–4325, DOI: 10.1016/j.gca.2008.11.032.
- 55 B. Mishra, M. Boyanov, B. A. Bunker, S. D. Kelly, K. M. Kemner and J. B. Fein, High- and Low-Affinity Binding Sites for Cd on the Bacterial Cell Walls of *Bacillus Subtilis* and *Shewanella Oneidensis*, *Geochim. Cosmochim. Acta*, 2010, **74**(15), 4219–4233, DOI: 10.1016/j.gca.2010.02.019.
- 56 B. Davis, R. Dulbecco, H. Eisen and H. Ginsberg, *Bacterial Physiology: Microbiology*, Harper and Row, Maryland, 2nd edn, 1973.
- 57 F. Liu, Q.-G. Tan, C. Fortin and P. G. C. Campbell, Why Does Cysteine Enhance Metal Uptake by Phytoplankton in Seawater but Not in Freshwater?, *Environ. Sci. Technol.*, 2019, **53**(11), 6511–6519, DOI: 10.1021/acs.est.9b00571.
- 58 J. Wingender, T. R. Neu and H.-C. Flemming, What Are Bacterial Extracellular Polymeric Substances?, in *Microbial Extracellular Polymeric Substances*, ed. J. Wingender, T. R. Neu and H.-C. Flemming, Springer Berlin Heidelberg, Berlin, Heidelberg, 1999, pp. 1–19, DOI: 10.1007/978-3-642-60147-7\_1.
- 59 T. R. Neu and J. R. Lawrence, Extracellular Polymeric Substances in Microbial Biofilms, in *Microbial Glycobiology: Structures, Relevances and Applications*, Elsevier, 2009.
- 60 J. R. Lawrence, G. D. W. Swerhone, U. Kuhlicke and T. R. Neu, In Situ Evidence for Microdomains in the Polymer Matrix of Bacterial Microcolonies, *Can. J. Microbiol.*, 2007, **53**(3), 450–458, DOI: 10.1139/W06-146.
- 61 H. Liu and H. H. P. Fang, Characterization of Electrostatic Binding Sites of Extracellular Polymers by Linear Programming Analysis of Titration Data, *Biotechnol. Bioeng.*, 2002, **80**(7), 806–811, DOI: 10.1002/bit.10432.
- 62 M. Stöckl, N. C. Teubner, D. Holtmann, K.-M. Mangold and W. Sand, Extracellular Polymeric Substances from *Geobacter Sulfurreducens* Biofilms in Microbial Fuel Cells, *ACS Appl. Mater. Interfaces*, 2019, **11**(9), 8961–8968, DOI: 10.1021/acsami.8b14340.
- 63 L. Hao, Y. Guo, J. M. Byrne, F. Zeitvogel, G. Schmid, P. Ingino, J. Li, T. R. Neu, E. D. Swanner, A. Kappler and M. Obst, Binding of Heavy Metal Ions in Aggregates of Microbial Cells, EPS and Biogenic Iron Minerals Measured in-Situ Using Metal- and Glycoconjugates-Specific Fluorophores, *Geochim. Cosmochim. Acta*, 2016, **180**, 66–96, DOI: 10.1016/j.gca.2016.02.016.
- 64 C. Wang, A. Lum, S. Ozuna, D. Clark and J. Keasling, Aerobic Sulfide Production and Cadmium Precipitation by *Escherichia Coli* Expressing the *Treponema Denticola* Cysteine Desulfhydrase Gene, *Appl. Microbiol. Biotechnol.*, 2001, **56**(3), 425–430, DOI: 10.1007/s002530100660.